15th European Signal Processing Conference (EUSIPCO 2007), Poznan, Poland, September 3-7, 2007, copyright by EURASIP

AN IMPROVED PARTIAL HAAR DUAL ADAPTIVE FILTER FOR SPARSE ECHO CANCELLATION

Patrick Kechichian and Benoît Champagne

Department of Electrical and Computer Engineering, McGill University
McConnell 602, 3480 University Street, Montréal H3A 2A7, Canada
email: patrick.kechichian@mail.mcgill.ca, champagne@ece.mcgill.ca

ABSTRACT

This paper proposes the use of a peak tendency estimator (PTE) based on Dezert Smarandache Theory (DSmT) and fuzzy inference to overcome two inherent limitations of a recently proposed partial Haar dual adaptive filter (PHDAF) for sparse echo cancellation. These limitations include the dependence of the PHDAF's performance on the echo path impulse response's bulk delay as a result of the lack of shift-invariance of the wavelet transform, and the PHDAF's difficulty in quickly tracking a new dispersive region after an abrupt change in bulk delay occurs. The improved PHDAF is analyzed in terms of its mean-square error (MSE) curves as well as its mean time to properly locate a dispersive regions under different SNRs. The simulations show that enhanced performance can be obtained using the proposed solutions at a minimal increase in computational cost.

1. INTRODUCTION

The presence of line (or network) echo is still commonplace in today's expanding communications infrastructure. Unlike acoustic echo, line echo is sparse, i.e.: the echo path impulse response contains a small number of non-zero coefficients, referred to as the dispersive region. Line echo is usually caused by an impedance mismatch, e.g. at the hybrid which converts the twisted-pair subscriber loop into a four-wire connection, where each pair of wires is separately used for transmit and receive signals. As a result of this mismatch, some of the transmitted signal leaks into the caller's receive path in the form of a reflection [1].

As the distance between two callers increases (delay $>$ 16 ms), the reflected signal becomes a distinct echo that can severely impede a conversation. The situation is worst for long distance calls routed via satellites due to the long round-trip echo delay, which can reach up to 600 ms. The coding and signal processing functions of newer digital technologies, designed to provide improved voice quality, in effect introduce extra processing delays into the echo path which render the echo problem even more predominant. Recent advancements, such as the deployment of Voice over Internet Protocol (VoIP) telephones, highlight the need to develop better echo cancellers for sparse line echo.

Recently, Bershad and Bist [2] have proposed a novel way of cancelling sparse echo, using a coupled configuration consisting of two short adaptive filters. Unlike Duttweiler's echo canceller [3], which requires the design of complex bandpass filters, the method in [2] uses a partial Haar wavelet transform, which is simple and just as amenable to a digital implementation. In this new method, referred to here as the Partial Haar dual adaptive filter (PHDAF), the first adaptive filter operates on a subset of input Haar coefficients, and is used by a peak delay estimator to determine the location of the echo path's dispersive region. The second adaptive filter is then centred around this location to actually cancel the echo in the time domain. In cases where the bulk delay is very large and a traditional echo canceller would require a large number of filter taps, the PHDAF provides a significant reduction in computational and memory requirements. In addition, by reducing the number of filter taps to an amount necessary to model the dispersive region, the convergence speed of the echo canceller is increased.

This paper presents a novel approach that introduces a peak tendency estimator (PTE) based on Dezert-Smarandache Theory (DSmT) and fuzzy inference to overcome two inherent limitations of the PHDAF in [2]. To cope with the shift-variant property of wavelet transforms, the PTE categorizes a peak's discernibility as either increasing or decreasing. If the peak is categorized as decreasing during a certain time interval, then a new set of transformed inputs is selected from a redundant form of the partial Haar transform and used to drive the partial Haar adaptive filter. The PTE is also used to improve the tracking performance of the coupled echo canceller in situations where an abrupt change in an echo path impulse response's bulk delay occurs. In simulation experiments using normalized least mean squares (NLMS) adaptation, the proposed amendments to the original PHDAF are shown to yield significant performance gains at a minimal additional computational cost.

2. BACKGROUND AND PROBLEM FORMULATION

2.1 Previous Work

The structure of the PHDAF proposed in [2] is shown in Fig. 1. The upper branch, consists of a partial Haar transform matrix denoted by $\mathbf{H}_q$ of size $q \times N$ and a length-q ($\leq N$) partial Haar adaptive filter. The term partial Haar reflects the fact that the transform only consists of a subset of Haar basis vectors of cardinality $q = 2^j$, corresponding to scale index j. These basis vectors span the sample interval of length N, which is set to match the maximum length of the unknown echo path impulse response. At time n, a new sample $u(n)$ is shifted into the input data vector of length N and a new transformed input vector $\mathbf{z}(n) = \mathbf{H}_q\mathbf{u}(n)$ of length q is calculated.

In this work, the partial Haar adaptive filter $\mathbf{v}(n)$, of length q, is updated by means of the NLMS algorithm, i.e.

$$\mathbf{v}(n+1) = \mathbf{v}(n) + \mu\|\mathbf{z}(n)\|^{-2}e_H(n)\mathbf{z}(n) \qquad (1)$$

where μ and $e_H(n)$ denote the step size and error signal, respectively. The peak delay estimator tracks the location of the dispersive region by locating the peak magnitude of $\mathbf{v}(n)$. It is shown in [2] that provided the input samples are uncorrelated, the Wiener solution of the partial Haar adaptive filter converges to the partial Haar transform of the Wiener filter for $\mathbf{u}(n)$, i.e. $\mathbf{v}_o = \mathbf{H}_q\mathbf{w}_o$, which can be seen as a compressed version of the true echo path impulse response. In addition, by independence theory assumptions, it can be shown that as the number of input samples increases, the updates of the partial Haar tap-weights become uncorrelated [2].

In the lower branch of the PHDAF, the estimated location of the dispersive region is used to offset a short time-domain filter $\mathbf{w}(n)$ of length L so that it is properly centred around the dispersive region. The value of L is set to match the longest expected dispersive region in the echo path. Once the partial Haar adaptive filter's peak location is properly estimated (initially, jitter in the peak delay estimate can occur), the short time-domain adaptive filter can converge to the dispersive region and thus cancel the echo signal $d(n)$. It is shown in [2] that the greater the steady-state peak magnitude of $\mathbf{v}(n)$, the quicker the short time-domain filter can be centred, and therefore, the faster the PHDAF can cancel

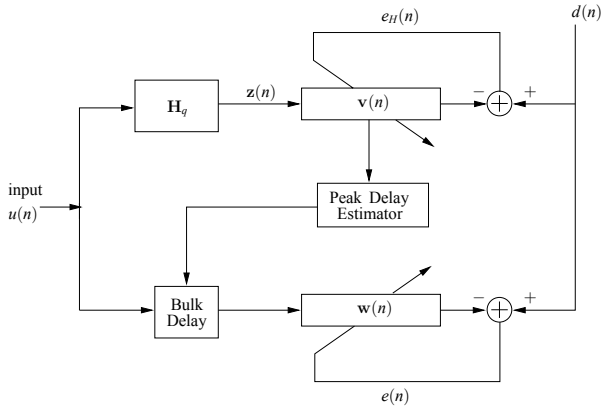

Figure 1: Coupled echo canceller.

2.2 Limitations

The simulation results in [2] show that the PHDAF may provide a drastic increase of the echo canceller's convergence speed in general, while keeping computational complexity low. However, our own experiments show that in certain specific cases, the PHDAF can require an extremely large number of input samples to converge. A related tracking problem may also be observed with the PHDAF after a sudden change in the true echo path impulse response.

The lack of shift-invariance of wavelet transforms can greatly affect the time required by the peak delay estimator to properly locate the dispersive region. For a wavelet transform whose basis vectors have a time-support of length $M = N/q$, the resulting discrete wavelet transform is periodically shift-invariant with a period equal to M. As a result, depending on the bulk delay of a given echo path impulse response, there exist *M unique* partial Haar transformed Wiener solutions. Furthermore, the respective peak magnitudes of each of these transformed impulse responses can be different, and consequently the amount of time it takes the peak delay estimator to correctly estimate the location of a dispersive region varies. For example, if the steady-state peak magnitude is comparable to or smaller than neighbouring coefficient noise, then the peak delay estimator will be unable to properly locate it. This can significantly affect the overall convergence speed of the coupled echo canceller. One of the goals of this paper is to propose solutions to amend the above situations, and therefore increase the robustness of the coupled echo canceller.

The promising results in [2] only represent the case when the partial Haar adaptive filter has been initialized to zero, i.e. $\mathbf{v}(0) = \mathbf{0}$, and the echo path is stationary. When an abrupt change in the echo path impulse response occurs, in particular a change in bulk delay, the mean time to locate the new dispersive region can be much longer. Unlike the zero-initialization case, where a peak only has to compete with neighbouring coefficient noise, in the case of a sudden change in bulk delay, the new peak also has to compete with the residual of older peaks.

In the next section, we look at ways to circumvent these two fundamental problems.

3. IMPROVING THE COUPLED ECHO CANCELLER

3.1 Redundant Partial Haar Transform

A consequence of the wavelet transform's lack of shift-invariance is the requirement of calculating the partial Haar transform of the input data block $\mathbf{u}(n)$ for every new input sample. The computational load for this operation can be shown to be on the order of $N-q$ arithmetic operations per iteration, which can be computationally expensive. Therefore, this paper opts for the use of a redundant form of the partial Haar transform which trades arithmetic operations with memory. Because this redundant partial Haar transform (RPHT) has a simple translational relationship with the input, it only requires calculating a single partial Haar coefficient every iteration.

Denoting the vector of RPHT coefficients by $\mathbf{s}(n)$ at time n,

$$\mathbf{s}(n) = [\mathbf{h}\mathbf{u}'(n), s(n-1), \ldots, s(n-N+1)]^T, \tag{2}$$

where $\mathbf{h}$ is a row vector of length N/q containing the non-zero portion of any row of $\mathbf{H}_q$ and $\mathbf{u}'(n) = [u(n), u(n-1), \ldots, u(n-N/q+1)]^T$. To extract the standard partial Haar transform from $\mathbf{s}(n)$, consider its $M = N/q$-fold polyphase decomposition,

$$S(z) = \sum_{l=0}^{M-1} z^{-l} \sum_{r} s(Mr+l) z^{-Mr}. \tag{3}$$

From (3) it is apparent that the transformed input vector $\mathbf{z}(n) = \mathbf{H}_q \mathbf{u}(n)$ corresponds to the first ($l = 0$) polyphase component of $S(z)$, while the remaining components represent $\mathbf{z}(n-1)$ down to $\mathbf{z}(n-N/q+1)$. In other words, the remaining polyphase components represent the transform vectors of input samples delayed by l sample(s). Therefore, driving the partial Haar adaptive filter with a specific polyphase component of $S(z)$, results in the filter's convergence to one of N/q solutions, each with its unique peak magnitude. In what follows, the term *context* will denote the polyphase component of $S(z)$ that is being used to drive the partial Haar adaptive filter to one of its N/q solutions.

3.2 Suboptimal-Context Escape Algorithm

The suboptimal-context escape algorithm (SCE) [4] developed in this section consists of two components: a peak tendency estimator (PTE) that models and categorizes a peak's discernibility, and a decision-making unit that decides when the current context should be changed in the event that a peak's discernibility is poor.

A) Peak tendency estimator (PTE):

The peak discernibility measure proposed here is calculated as follows: a) partition the partial Haar filter coefficients into three contiguous groups of roughly the same size, b) find the maximum peak magnitude for each of the three groups. The global maximum is found by selecting the maximum among the three maxima. The peak discernibility measure (or PDM) at time n is defined as

$$\mathrm{PDM}(n) = 1 - c_{\min}(n)/c_{\max}(n), \tag{4}$$

where $c_{\min}(n)$ is the minimum among the three maxima found at time n, and $c_{\max}(n)$ corresponds to the global maximum around which the short time-domain filter is centred (PDM(n) = 0, if $c_{\max}(n) = 0$).

The PTE uses DSmT and fuzzy inference, similar to [8], to track and categorize a peak's discernibility as increasing or decreasing. The adopted system makes use of two discernibility models as shown in Fig. 2. The first model corresponds to a PDM that increases over time with a transition $S \to S \to L \to L$, and eventually results in the proper detection of a dispersive region (S and L denote small and large discernibilities, respectively) . The second model corresponds to a decreasing discernibility with a transition $L \to L \to S \to S$, which can be used to detect filter-tap noise. The respective rule-bases and fuzzy graphs for each model are shown in Table 1 and Table 2. The fuzzy graphs are constructed using [5]

$$\max_{x \in \mathscr{X}}(\mu_{A_i \times C_i}(x)) = \max_{x \in \mathscr{X}} \min(\mu_{A_i}(x), \mu_{C_i}(x)). \tag{5}$$

where $\mathscr{X}$ denotes the permissible PDM values and equals $[0,1]$. Fuzzy inferences are made using Zadeh's max-min compositional rule [6] ($\mathscr{X} = \mathscr{Y}$ in this case),

$$\mu_{C'}(y) = \max_{x \in \mathscr{X}} \min_{i}(\mu_{A'}(x), \mu_{A_i \times C_i}(x,y)), \qquad y \in \mathscr{Y}. \tag{6}$$

The power of fuzzy inference lies in the fact that inferences can be made even when rules are only

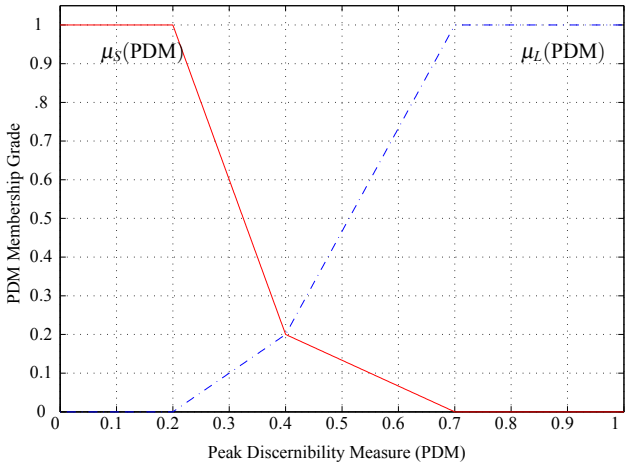

Figure 2: Fuzzy interface including small and large membership functions.

Table 1: Fuzzy Rule Bases

Rule No.	Increasing PDM
1:	If PDM(n) = S then PDM($n+1$) = S
2:	If PDM(n) = S then PDM($n+1$) = L
3:	If PDM(n) = L then PDM($n+1$) = L
Rule No.	Decreasing PDM
1:	If PDM(n) = L then PDM($n+1$) = L
2:	If PDM(n) = L then PDM($n+1$) = S
3:	If PDM(n) = S then PDM($n+1$) = S

At time n, the peak magnitude is characterized by the pair of fuzzy PDM values corresponding to the two models $\boldsymbol{\mu}^{\text{inc}}(n|n)$ and $\boldsymbol{\mu}^{\text{dec}}(n|n)$, where ($M$ = inc or dec)

$$\boldsymbol{\mu}^{M}(n|n) = [m(S), m(S\cup L), m(L), m(S\cap L)]^{M}. \tag{7}$$

The terms $m(\cdot)$ denote the basic belief masses (bbm) used within the DSmT framework. Using the matrix form of Zadeh's max-min rule [6], a state prediction of each model can be obtained,

$$\boldsymbol{\mu}^{M}(n+1|n) = \boldsymbol{\mu}^{M}(n|n) \circ \mathbf{G}^{M}, \tag{8}$$

where $\circ$ denotes a form of vector-matrix multiplication where multiplication and addition operations are replaced by the min and max operators, respectively. Each $\boldsymbol{\mu}^{M}(n+1|n)$ requires normalization for use in the DSmT combination step.

Table 2: Fuzzy graphs corresponding to two models of peak discernibility.

(a) Increasing discernibility, $\mathbf{G}^{\text{inc}}$

$n \to n+1$	S	$S\cup L$	L	$S\cap L$
S	1	0	1	0
$S\cup L$	0	0	0	0
L	0.2	0	1	0
$S\cap L$	0	0	0	0

(b) Decreasing discernibility, $\mathbf{G}^{\text{dec}}$

$n \to n+1$	S	$S\cup L$	L	$S\cap L$
S	1	0	0.2	0
$S\cup L$	0	0	0	0
L	1	0	1	0
$S\cap L$	0	0	0	0

At time $n+1$, a new vector of fuzzy PDM values is obtained from Fig. 2, i.e. $m_{n+1} = [m(S), m(S\cup L), m(L), m(S\cap L))]$ where

$$\begin{aligned} m_{n+1}(L) &= \mu_L(PDM(n+1)) && (9)\\ m_{n+1}(S) &= \mu_S(PDM(n+1)) && (10)\\ m_{n+1}(S\cup L) &= 1 - m_{n+1}(S) - m_{n+1}(L). && (11) \end{aligned}$$

This new input is separately combined with the predictions $\boldsymbol{\mu}^{\text{inc}}(n+1|n)$ and $\boldsymbol{\mu}^{\text{dec}}(n+1|n)$ using the DSmT rule of combination

$$m_{\text{upd}}(C) = \sum_{\substack{A,B\in D^{\Theta},\\ A\cap B = C}} m_1(A) m_2(B), \tag{12}$$

to obtain the updated fuzzy state vectors $\boldsymbol{\mu}^{\text{inc}}(n+1|n+1)$ and $\boldsymbol{\mu}^{\text{dec}}(n+1|n+1)$. Here, $D^{\Theta} = \{S, L, S\cap L, S\cup L\}$ denotes the hyper-power set.

B) Decision-making unit:

Making a decision about the peak magnitude's tendency then involves converting each set of updated bbms into their Pignistic probabilities P^{M} [7],

$$\begin{aligned} P^{M}\{S\} &= m_{\text{upd}}(S) + 0.5 m_{\text{upd}}(S\cup L) + 0.5 m_{\text{upd}}(S\cap L) && (13)\\ P^{M}\{L\} &= m_{\text{upd}}(L) + 0.5 m_{\text{upd}}(S\cup L) + 0.5 m_{\text{upd}}(S\cap L). && (14) \end{aligned}$$

At any time instant, a decision about the correct behavioural model is based on the model with the smallest entropy given by

$$H^{M}_{\text{pig}}(P^{M}) = -\sum_{A\in\{S,L\}} P^{M}\{A\} \ln(P^{M}\{A\}), \tag{15}$$

where $P^{M}\{A\}\ln(P^{M}\{A\}) = 0$ for $P^{M}\{A\} = 0$.

Escaping a suboptimal context, however, also requires deciding when to act on the information provided by the PTE. The approach used here consists of a schedule of N/q non-decreasing trial periods $\boldsymbol{\tau} = \{\tau_1, \ldots, \tau_{N/q}\}$ ($\tau_1 \le \tau_2 \le \ldots \le \tau_{N/q}$) to sequentially test each of the N/q contexts and is based on some prior knowledge about the amount of time required by the peak delay estimator to correctly locate a peak in different contexts. A schedule of non-decreasing trial periods ensures that the number of yet unattempted contexts that can successfully lead to a correct estimate of the peak delay increases after each failed attempt. At the same time, beginning the schedule with shorter waiting times escapes any suboptimal contexts earlier in the peak delay estimation process, while at the same time successfully staying in optimal contexts.

To summarize, the SCE algorithm begins by monitoring the peak tendency using the smallest trial period, τ_1. If the peak tendency is classified as decreasing for a period of time greater than this trial period and jitter occurs in the peak delay estimate, then the filter is reset to zero and a new context is attempted for the next trial period. This is repeated until the peak delay is correctly estimated. If all contexts have been attempted unsuccessfully, then the process is repeated beginning with τ_2.

3.3 Improved Tracking

Changes in an echo path impulse response can be associated with a change in the bulk delay, or a phase roll, where the impulse response coefficients change signs. The tracking of a dispersive region after an abrupt change in the echo path impulse response can be seen as a competition between filter coefficient magnitudes.

The proposed improved tracking (IT) algorithm [4] is based on the following observation about the PHDAF. When the partial Haar adaptive filter is initialized to zero, a peak's magnitude only has to compete with the low-magnitude coefficient noise of the surrounding taps, which makes its dete

Table 3: Number of arithmetic operations per iteration - single dispersive region

	PTE	SCE	IT	PHDAF
Add.	17	18	18	$2q+2L+N/q+1$
Mult.	18	18	18	$2q+2L+6$
Div.	3	3	3	1
Comp.	11	16	22	0

abrupt change in the echo path impulse response, however, a new peak might have to compete with the decreasing magnitude of an old peak. Therefore, although the echo path impulse response has changed, the peak delay estimator will take longer to find the peak corresponding to the new impulse response.

After an abrupt change in the echo path impulse response occurs, one finds that although the location of the new peak as well as its steady-state magnitude is unknown, the new steady-state magnitude of an old peak is approximately zero. Therefore, if a decrease in the current peak's magnitude is detected (which usually signals a change in the echo path impulse response), the entire partial Haar filter can be reset to $\mathbf{v}(n) = \mathbf{0}$. This is a feasible solution because the partial Haar filter is not being directly used to cancel echo and allows the new peak to solely compete with the low-magnitude coefficient noise of its neighbouring taps instead of the decreasing magnitude of the previous peak. As a result, the performance gains obtained in [2] in the stationary case can be extended to cases where abrupt changes in the echo path impulse response occur.

In order to prevent the IT algorithm from constantly resetting the partial Haar adaptive filter, the reset operation should only be performed every T_{RS} samples. In addition, a reset is only deemed necessary when a decrease in magnitude is detected for a peak whose tendency has been in an *increasing* state for an amount of time greater than T_{inc}. It is usually the case that $T_{RS} < T_{\text{inc}}$.

Adaptive filter coefficients are known to display a form of Brownian motion around the optimal solution [9] which can cause the IT algorithm to falsely detect a change in the impulse response. In order to prevent these false alarms, the algorithm also stores the position of the previous peak before resetting the filter, and feeds this position to the bulk delay unit. Once the new peak tendency has been increasing for an amount of time equal to T_{inc}, the algorithm begins using the location of the new peak to centre the short time-domain filter. An advantage of the IT algorithm is that it can also be integrated with the SCE algorithm.

3.4 Computational Complexity

The bulk of the SCE and IT algorithms' computational complexity lies with the PTE. Table 3 shows the number of arithmetic operations per iteration required by the PTE, the SCE, and IT echo canceller (which includes the SCE). Since only the incremental increase in complexity over the PHDAF is of interest here, the complexity values of the first three columns of Table 3 (PTE$\supset$ SCE-PHDAF$\supset$ IT-PHDAF) do not include the complexity associated with the PHDAF, while the values in the second and third columns of Table 3 include the values of their left-hand column.

Arithmetic operations associated with the PTE are drastically reduced since many bbm terms such as $m_{n+1}(S \cap L)$ and $m_{\text{pred}}(S \cup L)$, are zero throughout the PTE's operation. The two logarithmic operations related to calculating the Pignistic entorpies can also be eliminated since only the relative entropy is required. An alternate measure that preserves the relationship between the two Pignistic entropies and requires only a single comparison operation is given by $\tilde{H}^M_{\text{pig}} = \min(P^M\{S\}, P^M\{L\})$. Therefore, as an example, letting $N = 1024$, $q = 256$, and $L = 128$, the percentage increase in complexity when using the IT algorithm is $61/1548 = 3.94\%$, which is an acceptable amount.

4. COMPUTER SIMULATIONS

4.1 Methodology

The set of hybrid impulse responses used in the following simulations are taken from Annex D of the ITU-T G.168 Recommendation for digital network echo cancellers [10]. There are eight impulse responses $m_i(n)$ (for $i = 1, 2, \ldots, 8$) of lengths L_i that range from 64 to 128 samples at 8 kHz. It is assumed that $m_i(n) = 0$ for $n \notin \{0, 1, \ldots, L_i - 1\}$ and the echo return loss is 15 dB.

An input data vector of length $N = 1024$ with a partial Haar adaptive filter of length $q = 256$ and a schedule $\boldsymbol{\tau} = \{150, 250, 300, 400\}$ is used, unless stated otherwise. At the beginning of each run, the input data vector is initialized with the first N input samples of $u(n)$, a white zero-mean Gaussian process with unit variance. The additive measurement noise $v(n)$ is also a white Gaussian process, uncorrelated with the input, of zero-mean and variance $\sigma_v^2 = 10^{-\text{SNR}/10}$. The SNR is set to 30 dB, unless stated otherwise. The PHDAF and proposed algorithms will all operate with their partial Haar and short time-domain adaptive filters utilizing the NLMS algorithm with a step-size $\mu = 1$. In addition, the partial Haar NLMS update equation is normalized with $\|\mathbf{u}(n)\|^2$. The initial context is set to 1, which corresponds to no shifting of the partial Haar basis vectors. The NLMS algorithm is used as a reference for comparison.

4.2 Context Escaping

Figures 3(a) and (b) show the learning curves corresponding to an echo path impulse response using ITU-T G.168 hybrid model $m_5(n)$ under the best and worst bulk delays (with respect to the initial context), respectively. The curves represent an ensemble of 200 runs for each simulation.

For the best-case bulk delay (Fig. 3(a)), both the SCE-PHDAF and PHDAF show identical learning curves reaching steady state at around $k = 750$ compared to the NLMS which converges at around $k = 5000$. Of course, this is related to the fact that the NLMS adapts a far larger number of coefficients (1024 compared to 128). For a worst-case bulk delay (Fig. 3(b)), the PHDAF never seems to reach steady-state, while the proposed SCE-PHDAF converges much faster, nearly as well as in the optimal case, requiring about $k = 1000$ samples to converge. Several observations can be made concerning the results in Fig. 3. First, the proposed algorithm adds flexibility to the PHDAF in that it does not get trapped in suboptimal contexts. At the same time the proposed algorithm remains in optimal contexts. This behaviour may significantly increase the convergence speed of the echo canceller, as observed.

In addition to learning curves, the mean time for each echo canceller (proposed and PHDAF) to correctly estimate the location of a dispersive region was compared for different SNRs. Each row in Table 4 consists of the average and standard deviation over 500 random runs by randomly selecting one of eight ITU-T G.168 hybrid impulse response with equal probability, and a uniformly selected bulk delay in the interval [0,895]. In all cases, the proposed algorithm finds the dispersive region faster (the mean time is smaller) and more consistently (the standard deviation is much smaller). Although both PHDAF and the proposed echo canceller display similar mean times to convergence at very low SNR, the standard deviation of the PHDAF is three times larger. This reveals the robustness of using a fixed schedule $\boldsymbol{\tau}$ together with a PTE for different values of SNR. Of course, if the SNR does not change much over a specific channel, then schedules can be constructed specifically for those cases.

4.3 Improved Tracking

For reasons of brevity, only one case in Fig. 4 will be considered here. In this scenario, an echo path impulse response's bulk delay abruptly changes from an optimal to a suboptimal delay with respect to the initial context.

Initially, both echo cancellers converge optimally. However, after the abrupt change in bulk

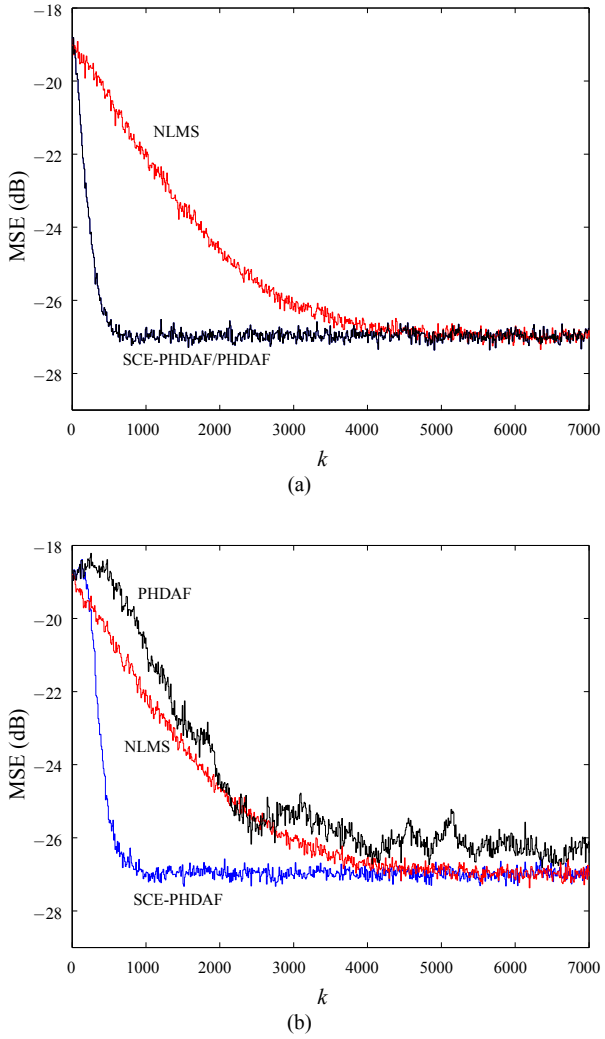

Figure 3: ITU-T hybrid response $m_5(k)$ learning curves using a: (a) best and (b) worst-case bulk delay for the initial context used. (SNR = 30 dB)

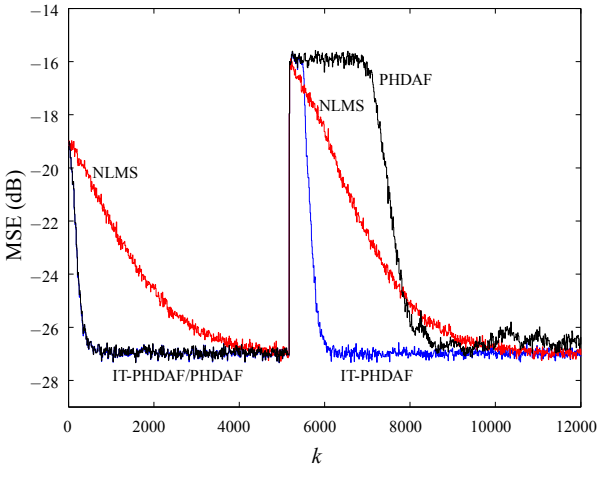

Figure 4: Tracking behaviour of the IT-PHDAF compared to the PHDAF and NLMS algorithm with a best-to-worst case change in bulk delay with respect to the initial context used (SNR = 30 dB).

Table 4: Comparison of mean times and standard deviation to correctly estimate the peak delay for different SNRs.

	SCE-PHDAF		PHDAF	
SNR (dB)	Mean	Std.	Mean	Std.
30	91.5	75.4	121.1	203.0
20	107.7	86.4	214.5	664.0
15	167.4	138.3	362.7	1067.7
10	421.4	387.1	531.7	1177.2

fewer samples to converge after a sudden change in the bulk delay. This result is supported by the plateau-region of the PHDAF's learning curve extending for almost 2000 samples in Fig. 4. The length of this plateau equals the amount of time it takes the new peak's magnitude (which is very small since the new bulk delay is suboptimal) to exceed the decreasing magnitude of the old peak.

5. SUMMARY AND CONCLUSION

The results obtained in this paper have shown that both suboptimal-context escaping or improved tracking (with suboptimal-context escaping) can considerably improve the performance of the PHDAF proposed by [2] without a significant increase in computational complexity. In [4], a distributed form of the SCE algorithm is developed to deal with the case of multiple dispersive regions.

REFERENCES

[1] S. V. Vaseghi, *Advanced Signal Processing and Digital Noise Reduction*. John Wiley and Sons Ltd., 1996.

[2] N. J. Bershad and A. Bist, "Fast coupled adaptation for sparse impulse responses using a Partial Haar Transform," *IEEE Trans. Signal Processing*, vol. 53, pp. 966–976, Mar. 2005.

[3] D. L. Duttweiler, "Subsampling to estimate delay with application to echo cancelling," *IEEE Trans. Acoustics, Speech, Signal Processing*, vol. 31, pp. 1090–1099, Oct. 1983.

[4] P. Kechichian, "On the Partial Haar Dual Adaptive Filter for Sparse Echo Cancellation," Master's Thesis. McGill University, Oct. 2006.

[5] G. J. Klir and B. Yuan, *Fuzzy Sets and Fuzzy Logic: Theory and Applications*. Prentice Hall, New Jersey, 1995.

[6] J.M. Mendel, "Fuzzy logic systems for engineering,"*Proc. of the IEEE*, vol. 83, pp. 345–377, Mar. 1995.

[7] J. Dezert, "Foundations for a new theory of plausible and paradoxical reasoning," *Int. Journal Inform. and Security*, vol. 9, pp. 13–57, 2002.

[8] A. Tchamova, T. Semerdjiev, and J. Dezert, "Estimation of target behavior tendencies using DSmT," in *Advances and Applications of DSmT for Information Fusion (Collected Works)*, J. Dezert and F. Smarandache, Eds. American Research Press, 2004.

[9] S. Haykin, *Adaptive Filter Theory*, 4th ed. Prentice Hall Inc., 2002.

[10] "Digital network echo cancellers, ITU-T Recommendations G.168," International Telecommunication Union, Tech. Rep., Aug. 2004.